

Republic of Iraq
Ministry Of Higher Education
And Scientific Research
University Of Baghdad
College Of Dentistry



Imaging of Salivary Glands

A Project Submitted to
The College of Dentistry, University of Baghdad,
Department of oral diagnosis in Partial Fulfillment for the
Bachelor of Dental Surgery

By:

Shaima Abd Al-Jabbar

Safa Essam Salleh

Supervised by:

lecturer Dr. Resha Jameel

B.D.S., M.Sc.

2022 A.D , April

1444 A.

سُورَةُ الضُّحَى

بِسْمِ اللَّهِ الرَّحْمَنِ الرَّحِيمِ

- وَالضُّحَى ①
وَاللَّيْلِ إِذَا سَجَى ②
مَا وَدَّعَكَ رَبُّكَ وَمَا قَلَى ③
وَلَلْآخِرَةُ خَيْرٌ لَّكَ مِنَ الْأُولَى ④
وَلَسَوْفَ يُعْطِيكَ رَبُّكَ
فَتَرْضَى ⑤
أَلَمْ يَجِدْكَ يَتِيمًا فَآوَى ⑥
وَوَجَدَكَ ضَالًّا فَهَدَى
وَوَجَدَكَ عَائِلًا فَأَغْنَى ⑦
فَأَمَّا الْيَتِيمَ فَلَا تَقْهَرْ ⑧
وَأَمَّا السَّائِلَ فَلَا تَنْهَرْ ⑩
وَأَمَّا بِنِعْمَةِ رَبِّكَ فَحَدِّثْ ⑪

Certification of the Supervisor

I certify that this project entitled " **Imaging of salivary gland** " was prepared by the fifth-year student **Shaima abd al-jabbar and safa essam** under my supervision at the College of Dentistry/University of Baghdad in partial fulfilment of the graduation requirements for the Bachelor Degree in Dentistry.

Supervisor's name: **lecturer Dr. Resha jameel**

Date

Dedication

I dedicate my project to my **family**, especially my **mother** and **father**, who sacrificed for us to light our way, and I thank my friend **Safa** for her hard work with me on this project day and night, befitting our mother college. I thank my dear supervisor for directing and guiding us and all the Department of Oral and Maxillofacial Radiology at the University of Baghdad, College of Dentistry. I dedicate my project to the spirit of **Dr. Alaa Salah**, who was the pinnacle of humanity.

Acknowledgment

First of all I'd like to thank **ALLAH** for helping me to complete this project then I would like to thank my supervisor **Dr. Resha Jameel** for guidance and advice, to **Prof. Dr.Raghad Abdul-Razaq**, dean of collage of dentistry, university of Baghdad for his continuous support for the students. Deep appreciation and respectful regards to **Dr.Bashar**, head of Oral Diagnosis department, College of dentistry, University of Baghdad, for facilitating the commencement of this project and providing all the support at his disposal.

List of content

Subjects	Page No.
Certification of the Supervisor	I
Dedication	II
Acknowledgements	III
List of Contents	VI
List of Figures	VI
List of Tables	VI
List of Abbreviations	VII
Introduction	1
Aim of study	3
Chapter one: Literature review	4
1.1 Salivary gland	4
1.1.1 Morphogenesis of salivary gland	4
1.1.2 Type of salivary gland	5
A-Parotid gland	5
B-Submandibular salivary gland	6
C-Sublingual salivary gland	7

D- Tubarial salivary gland	7
1.2 Chemistry of secretion and function of saliva	8
1.2.1 Chemistry of secretion	9
1.2.2 Component and Function of saliva	9
1.3 salivary gland disease	10
1.3.1 infection	10
1.3.2 Primary Sjögren's Syndrome	11
1.3.3 tumors	12
1.4 Imaging of salivary gland	13
A-Diagnostic Imaging	13
B- Projection imaging	13
1.4.1 High resolution Ultrasonography	15
1.4.2 Multidetector Computed Tomography MDCT	16
1.4.3 Magnetic Resonance Imaging	17
1.4.4 Nuclear Medicine	18
1.4.5 Sialography	19
1.4.6 Sialendoscopy	21
Chapter two: pervious study	22
Chapter three: conclusion and suggestions	26
References	27

List of figures

Figures	Pages No.
Figure(1) embryonic development of SMG and SL glands	4
Figure(2) parotid gland	6
Figure(3) submandibular salivary gland	7
Figure(4) Tubarial salivary gland	8
Figure(5) Standard mandibular occlusal and Periapical images	14
Figure(6) Panoramic Images shows Parotid sialolith	15
Figure(7) High-resolution ultrasonography image of the parotid gland	16
Figure(8) Axial soft-tissue algorithm multidetector computed tomography images	17
Figure(9) Axial soft-tissue algorithm multidetector computed tomography images	18
Figure(10) Nuclear Medicine	19
Figure(11) Sialography coupled with cone beam computed tomography	20
Figure(12) Sialendoscopy allows direct visualization of the salivary gland ducts	21

List of tables

Tables	Pages No.
Table(1) Components and function of saliva	10
Table(2) salivary gland tumors	13

List of Abbreviations

Abbreviations	
PG	Parotid gland
SL	Sublingual salivary gland
SMG	Submandiular salivary gland
EGF	Epidermal growth factor
FGF	Fibroblast growth factor
TGF-α	Transforming growth factor- α
PET	Positron emission tomography
AQP5	Aquaporin5
RNA	Ribonucleic acid
PSS	Primary Sjögren's syndrome
ER	Endoplasmatic reticulum
TNF	Tumor necrosis factor
BAFF	B cell activating factor
APRIL	A proliferation- inducing ligand
HRUS	High- resolution ultrasonography
MDCT	Multidetector computed tomography
MRI	Magnetic resonance imaging

TPT	Technetium pertechnetate
CBCT	Cone beam computed tomography
TIWI	T1 weighted images
T2WI	T2 weighted images
STIR	Short TI recovery images
MIP	Maximum intensity projection
SSD	Shaded surface display
3D	Three dimensional
VRI	Volume rendering techniques

Introduction

The salivary glands in mammals are exocrine glands that produce saliva through a system of ducts. Humans have three paired major salivary glands (parotid, submandibular, and sublingual), as well as hundreds of minor salivary glands (**Edgar et al., 2012**).

These Structures secreting fluid to facilitate feeding emerge progressively throughout evolution and can be found in very simple organisms and more complex species. In humans, major and minor salivary glands produce and secrete digestive fluids or protein-rich fluids. The three pairs of major salivary glands are responsible for the production and secretion of saliva in the oral cavity, whose moisturizing effect preserves oral hygiene and allows taste, speech and mastication (**Amano et al., 2012**). The parotid gland (PG) is mainly composed of serous acini-secreting α -amylase-rich saliva (**Dobrosielski-Vergona et al., 1993**). The sublingual gland (SL) secretes mucous, a viscous solution rich in mucins (**Korsrud et al., 1980**). The submandibular gland (SMG) is composed by a mixed population of acini with a mucous and serous function (**Smith et al., 1987**). These three major salivary glands account for more than 90% of salivary secretion. Minor salivary glands are distributed throughout the oral cavity, specifically in the labial and lingual mucosa, as well as palate and floor of the mouth. Saliva is an essential fluid for oral cavity maintenance and functionality (**Treuting, P.M et al., 2012**). Digestive enzymes within saliva initiate the digestion process, and at the same time, saliva acts as a lubricant of solid nutrition, thus helping its passage through the esophagus (**Kondo and Nakamoto, 2015**). By moisturizing the tongue and other tissues of the oral cavity, saliva has an essential role

in speech and taste sensitivity (**Matsuo et al., 2000**). It also balances the pH of the mouth, thus protecting the soft oral tissues and teeth from an extended exposure to an acidic environment. Saliva contains several signalling molecules, such as EGF, FGF, NGF and TGF- α , that are essential for the regeneration of oral and esophageal mucosa. Finally, the antibacterial and antifungal components of the saliva, such as lysozymes, immunoglobulin and lactoferrin, inhibit the progression of bacterial infection and dental caries.

Aim of study

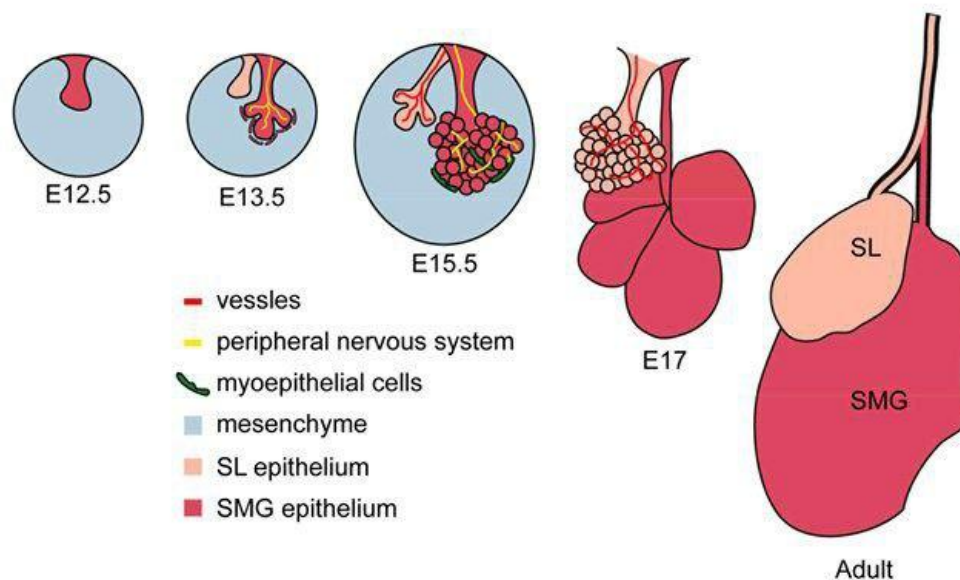
The aim of this study is to able the dentist to discover different methods in imaging of salivary glands for better diagnosis the diseases, and neoplasms that effect major and minor salivary gland in oral and maxillofacial region, and show the importance of different imaging modalities in diagnosis of salivary glands' diseases.

Chapter one: Literature review

1.1 Salivary gland

1.1.1 morphogenesis of salivary gland

Salivary glands originate from an epithelial placode during embryonic development (from E11 to E16 in mice and between the 4th and the 12th embryonic weeks in humans). The initial placode grows and extends into the underlying mesenchyme, acquiring a bud shape. The growing epithelial bud progressively stratifies with concentric layers each formed by a specialized cell type. During branching morphogenesis, the initial salivary bud divides into additional, independent buds that grow and cleave again, until the formation of an extensive arborization typical for the mature salivary gland (Jiménez-Rojo et al., 2012).



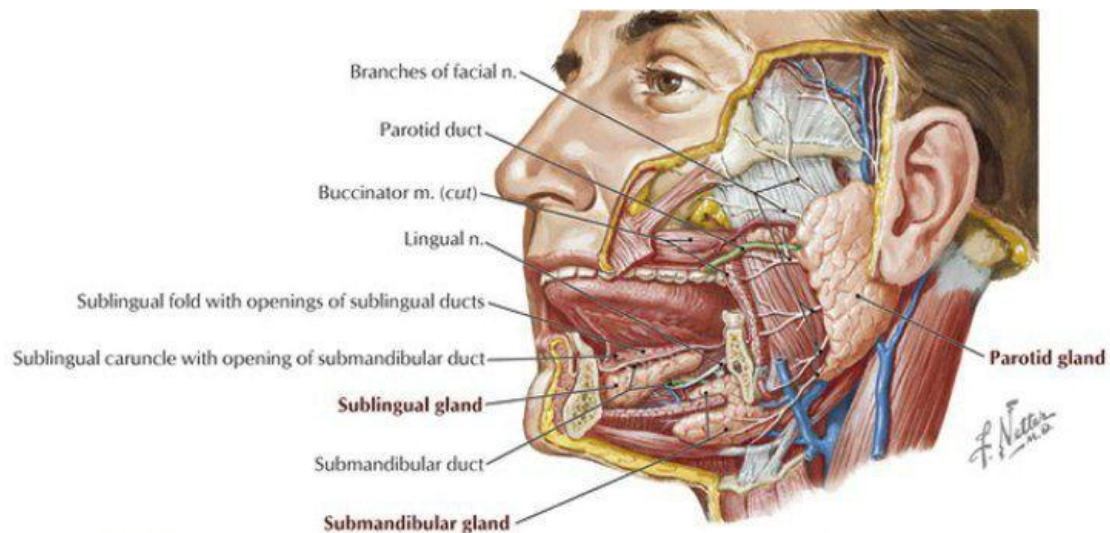
Figure(1)embryonic development of SMG and SL glands(Cristina et al., 2019).

A portion of the cells forming the outer epithelial layer of the buds differentiates into myoepithelial cells. They will then acquire smooth muscle characteristics and locate in direct contact with the acinar structure to regulate the release of secretion (**Gervais et al., 2016**). Inner epithelial cells differentiate further to acquire a distal (tips) or proximal (stalk) identity, which, in turn, evolves into acini or ducts, respectively (**Chatzeli et al., 2017**). Both epithelial and mesenchymal cells produce the basement membrane and stromal extracellular matrix. The composition of the extracellular matrix varies from region to region during branching, and bundles of collagen I, IV and bronectin are thought to directly control the maturation process.

1.1.2 Type of salivary gland

A- parotid gland

The two parotid glands are major salivary glands wrapped around the mandibular ramus in humans(**Bialek EJ et al., 2006**). These are largest of the salivary glands, secreting saliva to facilitate mastication and swallowing, and amylase to begin the digestion of starches(**Nanci A, 2018**). It is the serous type of gland which secretes alpha-amylase (also known as ptyalin)(**Holmberg and Hoffman, 2014**). It enters the oral cavity via the parotid duct. The glands are located posterior to the mandibular ramus and anterior to the mastoid process of the temporal bone. They are clinically relevant in dissections of facial nerve branches while exposing the different lobes, since any iatrogenic lesion will result in either loss of action or strength of muscles involved in facial expression(**Holmberg and Hoffman, 2014**). They produce 20% of the total salivary content in the oral cavity. Mumps is a viral infection, caused by infection in the parotid gland(**Hviid et al., 2008**).



Figure(2) parotid gland(Netter, 2019).

B- Submandibular salivary gland

The submandibular glands (previously known as submaxillary glands) are a pair of major salivary glands located beneath the lower jaws, superior to the digastric muscles(Bialek EJ et al., 2006). The secretion produced is a mixture of both serous fluid and mucus, and enters the oral cavity via the submandibular duct or Wharton duct. Around 70% of saliva in the oral cavity is produced by the submandibular glands, though they are much smaller than the parotid glands(Nanci A, 2018). This gland can usually be felt via palpation of the neck, as it is in the superficial cervical region and feels like a rounded ball. It is located about two fingers above the Adam's apple (laryngeal prominence) and about two inches apart under the chin.

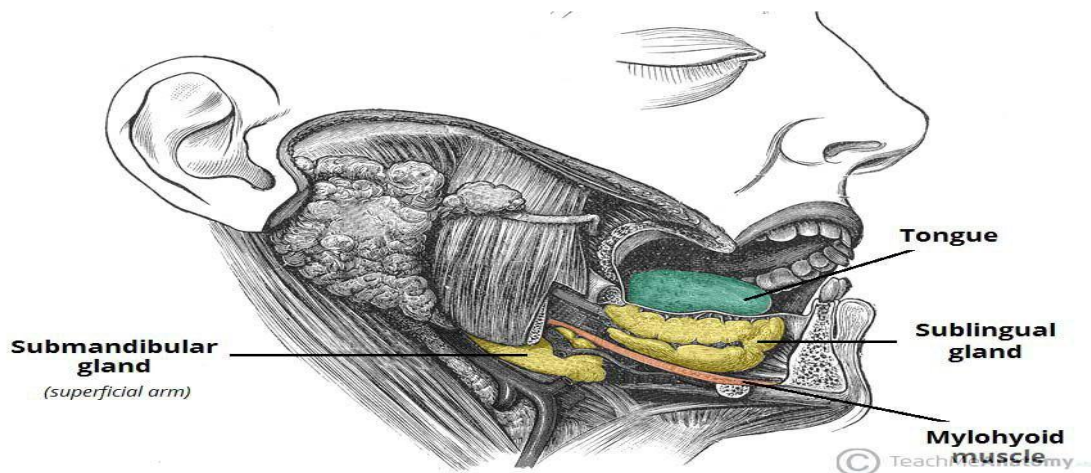


Figure (3) submandibular salivary gland(Jonathan et al.,2020).

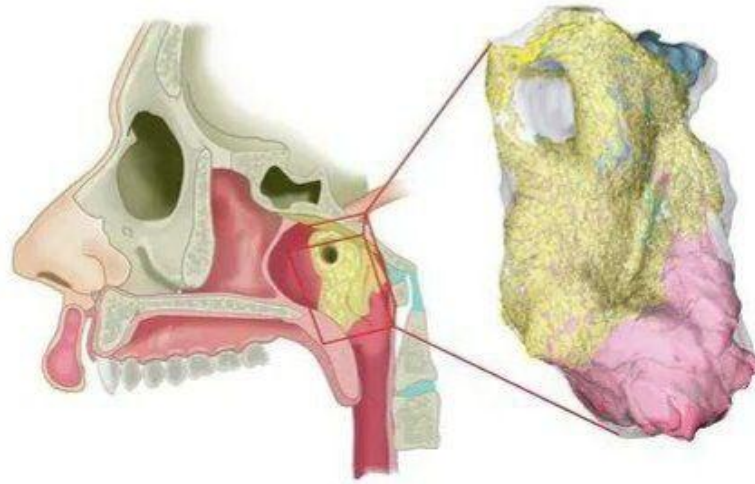
C-Sublingual salivary gland

The sublingual glands are a pair of major salivary glands located inferior to the tongue, anterior to the submandibular glands (Bialek EJ et al., 2006). The secretion produced is mainly mucous in nature, but it is categorized as a mixed gland. Unlike the other two major glands, the ductal system of the sublingual glands does not have intercalated ducts and usually does not have striated ducts, either, so saliva exits directly from 8-20 excretory ducts known as the Rivinus ducts. About 5% of saliva entering the oral cavity comes from these glands(Nanci A, 2018).

D- Tubarial salivary gland

The tubarial glands are suggested as a fourth pair of salivary glands situated posteriorly in the nasopharynx and nasal cavity, predominantly with mucous glands, and its ducts opening into the dorsolateral pharyngeal wall. The glands were unknown until September 2020, when they were discovered by a group of Dutch scientists using with prostate-specific membrane antigen PET-CT. This discovery may explain mouth dryness after radiotherapy despite the avoidance of the three major

glands. However, these findings from just one study need to be confirmed(Valstar et al., 2020)(Wu, Katherine J, 2020). On the other hand, an interdisciplinary group of scientists disagree with this new discovery. They believe that an accumulation of minor salivary glands has been described(Guntinas-Lichius et al., 2020).



Figure(4) Tubarial salivary gland(Diana, 2020).

1.2 Chemistry of secretion and function of saliva

Secretion itself is a combination of three events:

- (i) nervous cholinergic stimulation initiates uidltration from blood plasma to the acinar lumen.
- (ii) exocytosis of cytoplasmic granuli-containing proteins into the acinar lumen.
- (iii) mechanical contraction of the secretory end-pieces mediated by specialized myoepithelial cells(Cristina et al., 2019).

1.2.1 Chemistry of secretion

Primary saliva is initially produced and secreted in acinar cells. Epithelial cells of serous end-pieces are sealed between them via tight junction to preserve apical-basal polarity. This guarantees that electrolytes do not pass freely in between the cells, but require a system of ion-pumps and channels to rely regulate the intracellular and extracellular concentration of each electrolyte. Specifically, the Na/K ATPase pumps sodium out of the cell, which then accumulates in the intercellular space. Upon cholinergic stimulus, Ca^{2+} is released from intracellular storage sites (i.e., ER, mitochondria) and its concentration increases of 5–10-fold in the cytoplasm. This chemical change, in turn, opens the channels for Cl^- , which diffuses into the acinar lumen following its concentration gradient. Na^+ will then also translocate through the paracellular space to the lumen. Water from the adjacent capillaries will pass into the lumen by osmosis, both through paracellular flow specialized aquaporin channels (mainly AQP5) (Delporte et al., 2016).

1.2.2 Component and Function of saliva

Saliva is a very dilute fluid, composed of more than 99% water. Saliva is not considered an ultrafiltrate of plasma (Dowd FJ, 1999); initially, saliva is isotonic; it is formed in the acini, but it becomes hypotonic when it travels through the duct network.

- 1) Bicarbonates, phosphates, and urea act to modulate pH and the buffering capacity of saliva.
- 2) Macromolecule proteins and mucins serve to cleanse, aggregate, and/or attach oral microorganisms and contribute to dental plaque metabolism.

3) Calcium, phosphate, and proteins work together as an antisolubility factor and modulate demineralization and remineralization.

4) Immunoglobulins, proteins, and enzymes provide antibacterial action (Humphrey et al., 2001).

Salivary component	Function
Amylase and proteases	Digestion
Bicarbonate	Buffering
Calcium	Remineralization
Salivary antibodies and lactoferrin	Antimicrobial
Lysozyme	Hydrolysis of cell membrane
Mucine	Digestion, lubrication and pellicle formation .
Water	Mucosal integrity

Table(1) Components and function of saliva (Narendra, 2019).

1.3 salivary gland disease

1.3.1 Infection

Several viruses and bacteria infect the tissue of salivary glands in a specific manner. Endemic parotitis is due to infection of the mumps virus and lead to PG swelling and systemic symptoms. It is mainly affecting children in pre-scholar age and treatment is primarily symptomatic. The HIV virus can infect the PG and induce the formation of cystic lesions with surgical resection being the most common treatment procedure.

Hepatitis C and coxsackievirus are RNA-bound viruses, able to infect salivary glands and damage the host tissue, leading to xerostomia. One of the main routes of viral spreading is the gland secretion itself and thus transmission through saliva exchange is the major infection mode. Bacterial infection is very rare and mainly affects the PG in patients already debilitated by other conditions, such as diabetes, recovery after surgery or immunodeficiency. Therapeutic treatments reducing saliva flow help the establishment of bacterial colonies in the mucosa and increase the risk of infection, mainly from *Streptococcus* strains and *Staphylococcus aureus*. Mycobacter infection is more common in infants where it locally grows masses that might break the skin of the patient leaving scarring of the tissue. Non-controlled bacterial infection might spread beyond the gland borders and invade the deep space of the neck with possible serious complications including septicaemia. Chronic inflammation might also lead to sialadenitis, an accumulation of lymphocyte infiltrate in the duct system with consequent obstruction and hampering of the secretory system. Clinically, this results in xerostomia and local painful swelling (Wilson et al., 2014).

1.3.2 Primary Sjögren's Syndrome

Primary Sjögren's syndrome (pSS) is a systemic autoimmune disease affecting salivary and lacrimal glands. Often accompanying other immune system disorders (such as lupus and rheumatoid arthritis), its main effect is the loss of mucous membrane and moisture-secreting gland cells, resulting in xerostomia and xerophthalmia. Although the pathogenesis of the disease remains largely unknown, the role of the B-lymphocytes appears to be essential in the initiation of the disease. Members of the TNF superfamily (such as BAFF/APRIL) are produced not only by patrolling immune cells but also by the epithelial cells of the

salivary glands. Through these pathways, B-cells are activated and start to proliferate in an uncontrolled manner(Groom et al., 2002). Their pivotal role includes infiltration of the salivary glands to produce an ectopic germinal centre and local secretion of autoantibodies. The centre can grow independently from the surrounding tissue and can evolve in more complex diseases such as non-Hodgkin lymphoma(Chadburn et al., 2004).

1.3.3 tumors

Tumours originating in salivary gland tissue are often benign. In minor salivary glands, the most common clinical complication is the formation of mucus retention cysts, a non-malignant evolution of the altered tissue(Senthilkumar et al., 2014).

Type	Origin	Most common location	Metastasis
Mucoepidermoid Carcinoma	Excretory stem cells	PG	Yes, regional lymphnodes
Adenoid Cystic Carcinoma	Intercalated stem cells	minor SG	Yes, lungs
Acinic Cell Carcinoma	Intercalated stem cells	PG	
Polymorphous Adenocarcinoma	Intercalated ductal cells	Minor SG	Rarely Perineural lymphnodes
Squamous Cell	Excretory stem	PG, SMG	Neck region

Carcinoma	cells		
Non-Hodgkin lymphoma	Inltrating immune cells	PG	
Pleomorphic adenoma	Intercalated stem cells	PG	no

Table(2) salivary gland tumors(Alvi et al., 2019).

1.4 Imaging of salivary gland

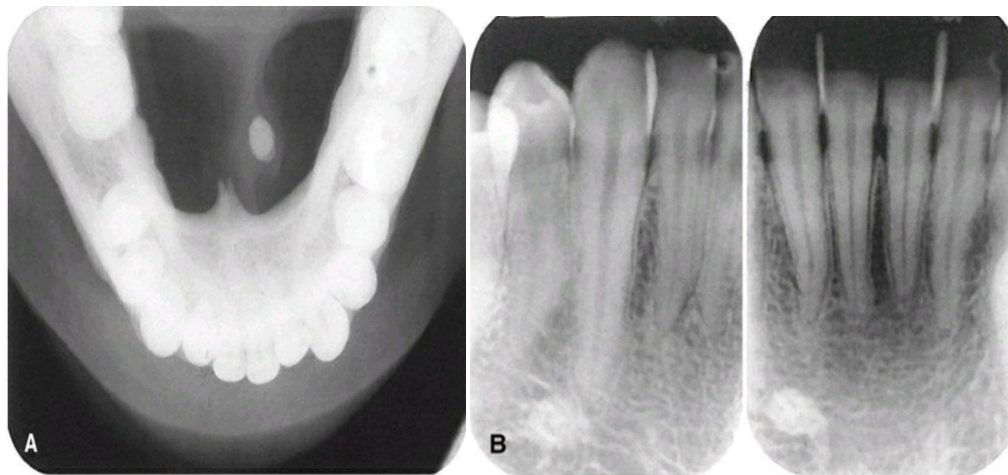
A- Diagnostic Imaging

Imaging is often used to diagnose and to plan management and follow-up of patients with salivary gland disorders. It provides crucial information regarding the nature of the disease affecting the salivary glands, the extent and severity of glandular involvement, and the effect on the surrounding structures. Many of the available imaging modalities have been used to image the salivary glands including projection radiography, high-resolution ultrasonography (HRUS), multidetector computed tomography (MDCT), magnetic resonance imaging (MRI), nuclear medicine, sialography, and most recently sialendoscopy(Abdel-Wahed et al., 2013).

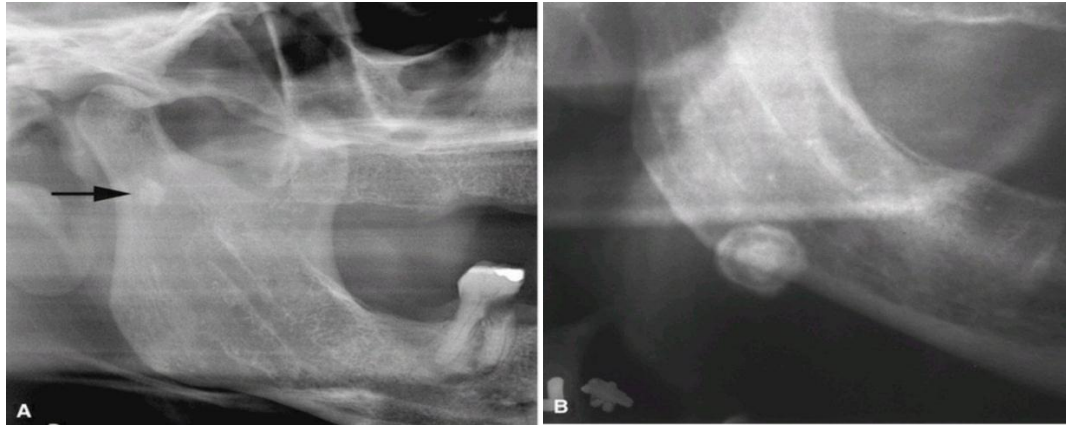
B- Projection imaging

Projection images, whether intraoral occlusal images or extraoral panoramic images, are helpful in identifying calcified sialoliths. Cross-sectional mandibular occlusal images are best used to identify submandibular duct sialoliths(Abdullah et al., 2013), whereas panoramic images may be used to demonstrate both parotid and submandibular sialoliths. Parotid sialoliths appear superimposed over the mandibular

rami superior to the occlusal plane, whereas submandibular sialoliths appear superior to the hyoid bone near the antegonial notch of the mandible(**Brown JE et al., 2002**). Therefore these images should be considered first when the patient presents with signs and symptoms suggestive of a sialolith such as swelling and pain just prior to or during mealtime(**Browne RF et al., 2001**). Some of the advantages of projection images are that they are readily available, are inexpensive, and subject the patient to a relatively low dose of radiation. In addition, they allow examination of osseous structures adjacent to the salivary glands. However(**Burke et al., 2011**), projection images do fail at identifying noncalcified sialoliths, which are estimated to account for 40% of all parotid sialoliths and 20% of all submandibular sialoliths(**Drage et al., 2000**).



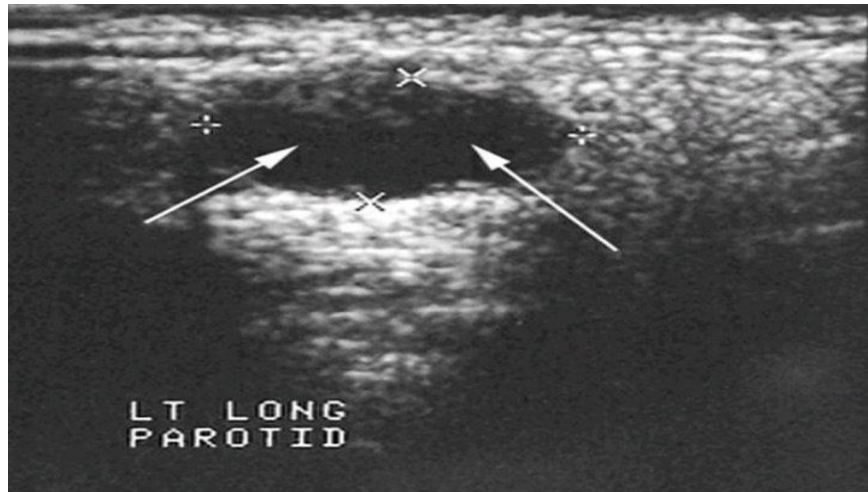
Figure(5)(A) Standard mandibular occlusal and (B) Periapical images demonstrating an oval- shaped radiopaque sialolith in a Wharton duct(**Saniav et al., 2019**)



Figure(6) ropped Panoramic Images. (A) Parotid sialolith superimposed over condylar neck (arrow) superior to the plane of occlusion. (B) Submandibular sialolith near the antegonial notch of the mandible. Note the concentric lamellar pattern characteristic of sialoliths(Sanjay et al., 2010)

1.4.1 High resolution Ultrasonography

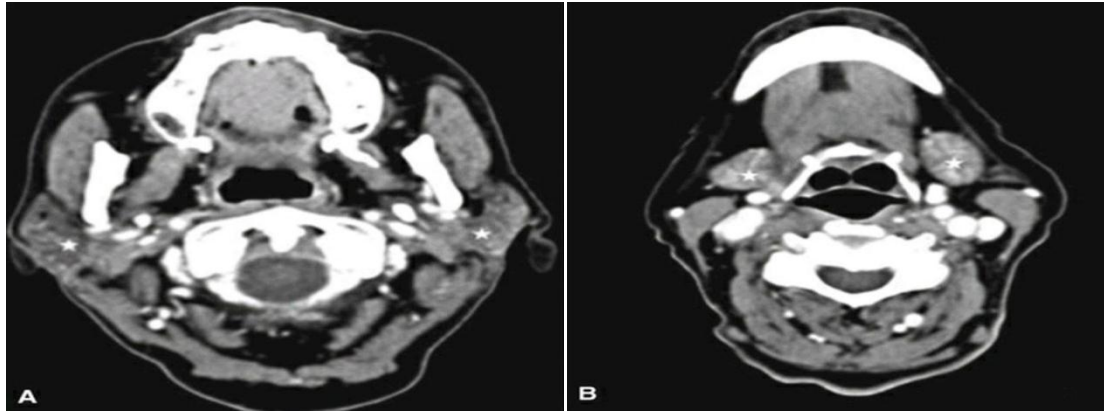
This technique may be used for the initial assessment of the parotid and submandibular glands, especially when an abnormality is located superficially. It may also be used to guide biopsies and further imaging choices. HRUS is helpful at differentiating cysts from neoplasms, and benign from malignant lesions (Fig7). HRUS has become more specific at detecting Sjögren syndrome, but it is still lacking in its ability to detect sialoliths. The major disadvantage of HRUS lies in its inability to detect deep salivary gland lesions, whereas its major advantage is its relative safety because it does not use ionizing radiation(**Drage et al., 2002**).



Figure(7) High-resolution ultrasonography image of the parotid gland demonstrating an echo-free mass with well-defined margins, which is typical of a cystic mass (arrows). (Courtesy Department of Radiology, Baylor University Medical Center, Dallas, TX 2020).

1.4.2 Multidetector Computed Tomography MDCT

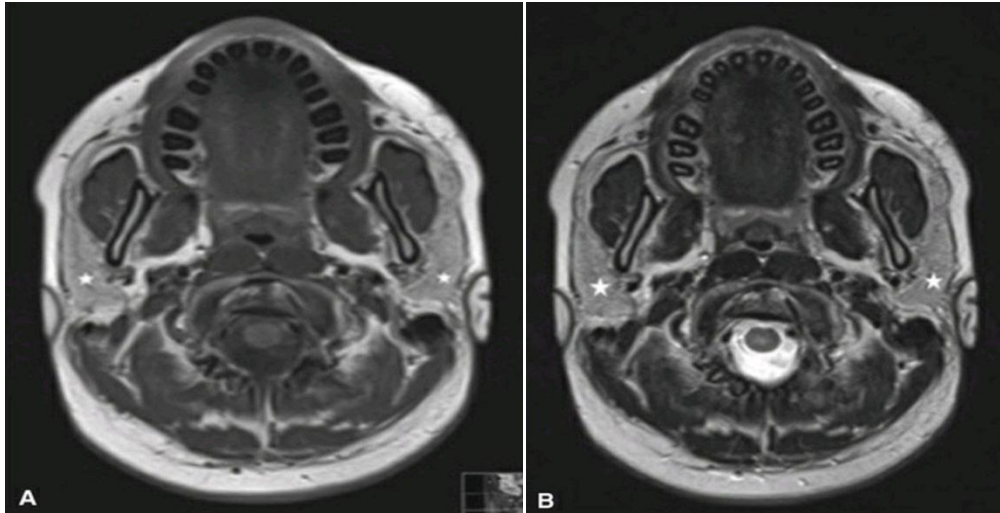
MDCT, displayed in both hard- and soft-tissue windows, is useful in evaluating not only the salivary glands but also the structures surrounding them (Fig. 8). This is especially true when the images are acquired after intravenous administration of a contrast agent that renders glandular tissues hyperdense relative to the surrounding fat and muscle(Jadu et al., 2014). MDCT imaging is used in cases when inflammation of the salivary glands is suspected because it demonstrates characteristic features such as peripheral enhancement, thickening of the subcutaneous tissue, and lymph node involvement, some or all of which can be seen in inflammation or neoplasia. Sialoliths are well depicted on MDCT images but only if they are relatively large and significantly calcified. Smaller, less-calcified sialoliths and ductal strictures are not well(Dreiseidler et al., 2010).



Figure(8) Axial soft-tissue algorithm multidetector computed tomography images (A) at the level of the parotid glands (stars) and (B) at the level of the submandibular glands (stars). Because the salivary glands have more fatty stroma than muscles, they appear less dense than adjacent muscles (Courtesy Dr. K. Khashoggi, Jeddah, KSA.)

1.4.3 Magnetic Resonance Imaging

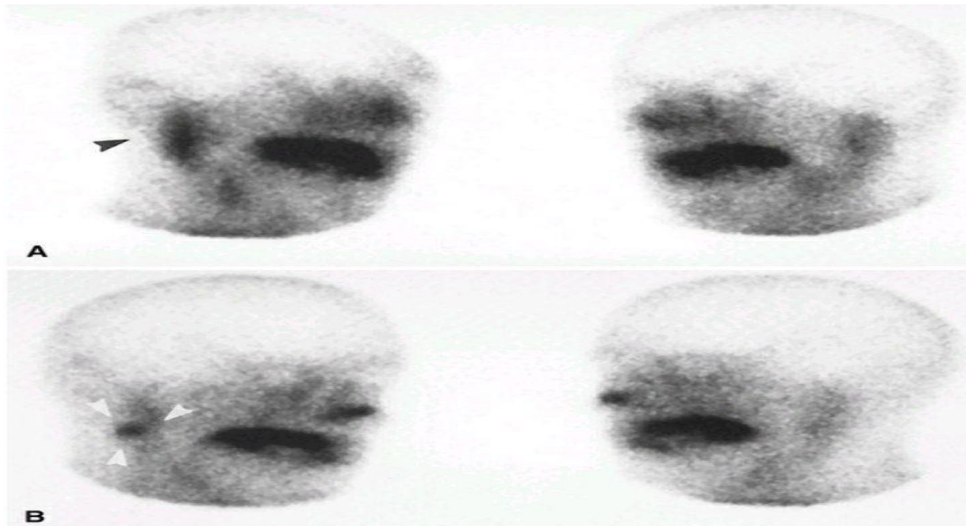
Although indications for MRI occasionally overlap with those of MDCT, MRI is the imaging method of choice for assessment of space-occupying lesions (cyst and neoplasms) of the salivary glands because of its superior soft-tissue contrast (Fig. 9). In addition, the use of intravenous gadolinium as a contrast agent makes MRI the imaging modality of choice for evaluation of intracranial and perineural spread of disease. Detection of sialoliths, particularly when calcified, is problematic in MRI because these calcific entities result in signal voids. Other disadvantages of MRI include long acquisition times, relatively poor spatial resolution, cost, and accessibility (MacDonald et al., 2009).



Figure(9) Axial soft-tissue algorithm multidetector computed tomography images. (A) T1-weighted image and (B) T2-weighted image displaying the hyperintense signal of the parotid glands (stars) relative to the adjacent muscle(Courtesy Dr. K. Khashoggi, Jeddah, KSA.)

1.4.4 Nuclear Medicine

Nuclear medicine examinations are functional examinations of the salivary glands. This modality takes advantage of the selective uptake of specific radiopharmaceuticals such as technetium 99m (^{99m}Tc)-pertechnetate (TPT) by the salivary glands when injected intravenously. This is followed by administration of a sialagogue evaluate the secretory capacity of the salivary glands. Pathosis may be determined on the basis of variations in the rate of TPT uptake or clearance. For example, Warthin tumor distinctively demonstrates reduced TPT clearance (Fig. 10)(Mande et al., 2014). Nuclear medicine is a highly sensitive technique that allows examination of all the major salivary glands at once; however, it lacks specificity and resolution which makes assessment of the salivary gland morphology difficult(Nahlieli et al., 2006)

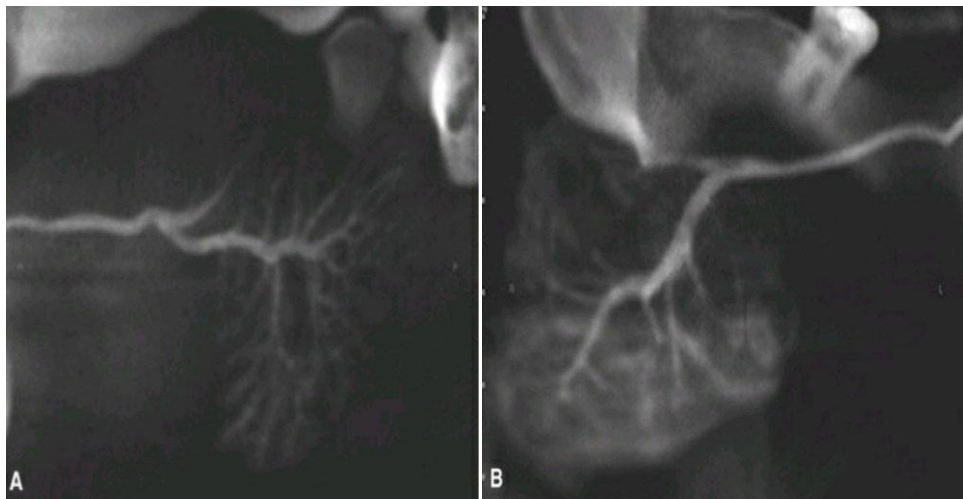


Figure(10) Nuclear Medicine. (A) Technetium 99m (^{99m}Tc)-pertechnetate (TPT) scan of the salivary glands (right and left anterior oblique views) demonstrates increased uptake in the right parotid gland (black arrowhead). (B) Nuclear medicine image obtained after administration of a sialogogue (lemon juice) demonstrates retention of TPT in the right parotid gland (white arrowheads). This is a typical presentation of a Warthin neoplasm.

1.4.5 Sialography

First performed in 1902, sialography is an imaging technique exclusively used for the parotid and submandibular salivary glands (Nahlieli et al., 2001). The technique involves infusion of the gland ductal system with an iodinated contrast agent, and then imaging the gland with projection imaging, fluoroscopy, MDCT, or cone beam computed tomography (CBCT). Sialography is the only imaging technique that can assess both the morphology of the parotid and submandibular glands in addition their function. The rate of clearance of the contrast agent from the gland, especially when prolonged, is used as an indirect indicator of reduced secretory function. MRI may be combined with sialography, but in these cases the patients' own saliva is used as a contrast agent and the imaging

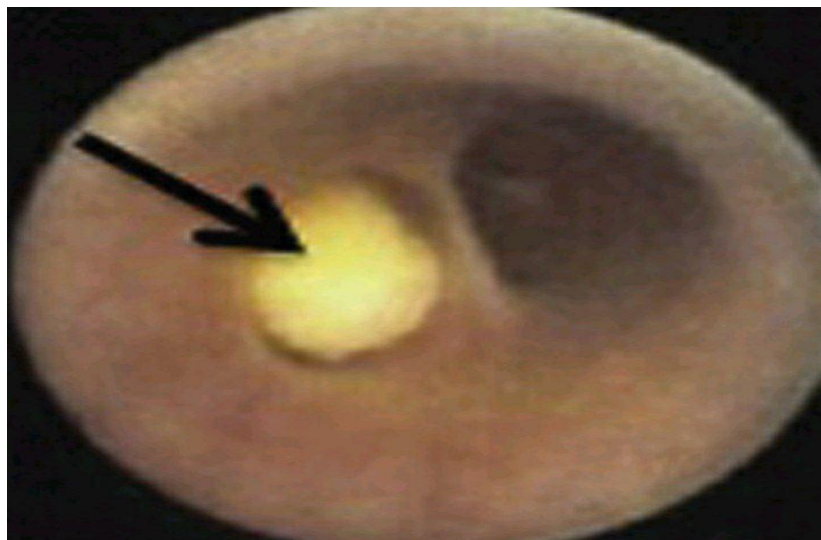
is done using heavily weighted T2 protocols(Ngu RK et al., 2007). The primary indication for sialography is chronic inflammatory conditions, especially when obstruction is suspected(Shahidi et al., 2014). There are two contraindications for sialography. The first of these is acute infection because injection of the contrast agent may disperse the infection into otherwise unaffected regions within the gland and cause further pain for the patient(Yousem et al., 2000). The second contraindication is an immediately anticipated thyroid function test because the iodine in the contrast agent may concentrate in the thyroid gland and interfere with the results of the test. Recently, sialography has been coupled with CBCT, and this coupling has resulted in three-dimensional images with submillimeter resolution and multiplanar capabilities that have revolutionized the visualization of the parotid and submandibular glands (Fig. 11).



Figure(11) Sialography coupled with cone beam computed tomography. (A) Corrected sagittal image of a normal left parotid gland illustrating the branching pattern of the ductal structures. (B) Corrected sagittal image of a normal right submandibular gland also illustrating the branching ducts. The outline of the gland body is displayed here due to filling of the acini with contrast material(Senior et al., 2010)

1.4.6 Sialendoscopy

Since its first use in the 1990s, this examination that involves direct visualization of the parotid and submandibular major ducts (Fig. 12) has transformed the diagnosis and management of obstructive conditions of these glands. The minimally invasive technique can be equipped with sialolith retrieval and stricture dilation tools that have enabled management of these common conditions with reported success rates greater than 95%. Acute inflammation is the only known contraindication for this relatively new technique because of the possible pain that may be elicited(El-Khateeb et al., 2011).



Figure(12) Sialendoscopy allows direct visualization of the salivary gland ducts. This particular image demonstrates a sialolith (arrow) in one of the branching ducts. (Courtesy Dr. F. Marchal, Geneva, Switzerland).

Chapter two: pervious study

Biatek et al., 2003: used US and conducted to estimate the utility of ultrasonography in diagnosis and differentiation of pleomorphic adenomas. In this study, was found from the group of 88 patients examined by ultrasound, who were referred because of the tumor in the pre-auricular area, submandibular area, or cheek, pleomorphic adenoma was finally diagnosed in 24 (with multiple recurrent tumors in 2 patients). Ultrasound was able to differentiate between benign and malignant lesions with 96% accuracy in this study. Predicting that the detected tumor was pleomorphic adenoma was possible with up to 84% accuracy. In 15 of 22 patients with primary pleomorphic adenoma, ultrasound guided fine-needle aspiration biopsy. High-resolution probes and harmonic imaging enabled demonstration of histopathologic heterogeneity of pleomorphic adenomas (in 16 primary tumors [73%]). Of primary pleomorphic adenomas, 95% (21/22) had 5 or fewer vessels detectable in the whole lesion. They concluded that the Modern ultrasound is highly valuable, useful, and reliable in differential diagnosis of tumors in the preauricular area, submandibular area, and cheek. It enables precise localization, measurements, and assessment of the structure of lesions. It may be the first and last imaging method needed to formulate the final diagnosis, or it may guide fine-needle aspiration biopsy. In many cases, ultrasound may also suggest the nature of the tumor.

(El-Rasheedy et al., 2021) The other study that utilized US and evaluate the role of ultrasound in the evaluation of salivary glands swellings in comparison with a computed tomography scan. In this study A total of 80 patients aged more than 1 year old with swellings affecting the salivary glands were collected from the out-patient clinic during the

period from February 2020 to February 2021. All patients underwent ultrasonography and computed tomography examination of the neck. All submandibular gland lesions presented with sialolithiasis (40 cases) (100%), and 20 cases (50%) of parotid gland swellings presented as inflammation without stone (16 cases (40%) of acute inflammation and 4 cases (10%) with recurrent inflammation), while 4 patients only presented as sialolithiasis. Neoplastic lesions were diagnosed in 16 cases of the parotid gland group. Stones less than 3 mm were detected only by computed tomography in 5 patients (12.5%) of the submandibular group. Twenty-eight cases (70%) with stones ranged in size between 3 and 6 mm. Only 11 cases (27.5%) with stones ranged in size more than 6 mm. Of the 16 parotid swellings diagnosed with neoplastic lesions, 14 parotid cases (87%) showed well-defined margins by computed tomography and ultrasonography. They concluded that the Ultrasound is the investigation of choice in salivary gland swellings. Computed tomography could be needed in certain cases such as deep parotid gland lesions or sialolithiasis with small stones in the ducts of the salivary glands. Computed tomography should be done in cases suspected of malignant salivary gland lesions.

(Oscar Hasson, 2010) was conducted to revisit and reintroduce sialography as an important tool for the assessment and diagnosis of salivary gland obstruction. In this study a sample of 30 consecutive patients undergoing sialography was selected. Parotid sialography was performed in 22 patients (12 females and 10 males). The patients undergoing parotid sialography presented with bilateral or unilateral enlargement or swelling. Submandibular sialography was performed in 8 patients (all males) who had presented with swelling and pain in the affected gland. They found Parotid sialography revealed 6 cases of

sialolithiasis without significant duct narrowing, 3 of narrowing and strictures of Stensen's duct without a sialolith, 3 glands with gland sialectasis, 1 parotid gland with intraglandular cyst-like duct degeneration, 1 of a parotid mass displacing Stensen's duct, and 1 gross dilation of duct. The findings of 7 parotid gland sialograms were normal. Submandibular gland sialography revealed the presence of sialolithiasis (single and multiple) in 4 patients, narrowing of the duct in 2, and normal findings in 2. so we concluded that the Sialography is a simple technique and an important tool for the assessment of salivary gland obstruction in patients presenting with sialadenitis.

(Ichiro et al., 2018) were performed To assess the correlation between conventional magnetic resonance (MR) imaging and MR sialography of parotid glands with salivary gland scintigraphy in patients with Sjögren's syndrome.

A retrospective study was conducted on eight patients with Sjögren's syndrome who underwent MR imaging and salivary gland scintigraphy. Conventional MR imaging techniques, such as T1-weighted images (T1WI), T2-weighted images (T2WI), and short TI inversion recovery images (STIR) were used for changes of fat signal in the parotid gland, while the MR sialography were used for ducts dilation of the parotid gland. Regarding scintigraphy, time-activity curves of each parotid gland were analysed. The salivary gland excretion fraction was defined as A (before stimulation test (counts/20 s)) and B (after stimulation test (counts/20 s)). They resulted from this study that the characteristic appearances of fat signal, the A/B of parotid gland with homogeneous intensity distribution (3.51 ± 0.75) was higher than that with heterogeneous intensity distribution (1.56 ± 0.66 , $P = 0.001$). Regarding MR sialographic stages, the A/B of parotid gland with stage 0 ($3.51 \pm$

0.75) was higher than that with stage 1 (2.03 ± 0.86 , $P = 0.009$) and with stage 2 (1.26 ± 0.25 , $P = 0.000$). they suggest that MR sialography of the parotid glands is a useful noninvasive tool for evaluating the decrease of salivary gland excretion in patients with Sjögren's syndrome.

Also, (Y Morimoto et al., 2002) were performed to evaluate the effectiveness of magnetic resonance (MR) sialography of parotid gland and/or submandibular gland ducts using three-dimensional fast asymmetric spin-echo (3D-FASE) sequencing. The objective was to make three-dimensional (3D) reconstruction images and virtual endoscopic views of the parotid gland ducts using MR sialography data sets of 3D-FASE sequences. We reviewed the MR sialography data sets with 3D-FASE sequencing of 10 control volunteers and six patients. Three-dimensional reconstruction images and virtual endoscopic views of the parotid gland and/or submandibular gland ducts were generated with maximum intensity projection (MIP), shaded surface display (SSD), and volume rendering techniques (VRT). The result was that the main parotid gland and/or submandibular gland ducts, large branches within the glands, and small branches were fairly well defined in a very short acquisition time on MR sialographic images with 3D-FASE sequencing in nine of the 10 healthy volunteers. The 3D-reconstruction images of the parotid gland ducts and/or submandibular gland ducts showed the entire length of the branch paths and complete images from all angles, and the virtual endoscopic views showed the endoluminal tracts of the main ducts and the large branches in nine. In the patient with Sjogren's syndrome, chronic sialoadenitis, and salivary calculi in the Wharton ducts, the MR sialographic images showed diffuse areas of punctate high signal intensity, dilatation of Stensen's duct, or stones of Wharton's duct, respectively. Furthermore, the 3D-reconstruction images of the salivary

gland ducts showed the stenoses and stones in the branch paths and complete images from all angles, and the virtual endoscopic views showed the stenoses and stones in the endoluminal tracts of the main and large branches. Our initial experience showed that virtual MR endoscopy could be performed to observe the endoluminal tracts of parotid and submandibular glands. They concluded that The clinical use of the virtual MR endoscopy for salivary gland ducts has not been established yet. Future applications of the 3D-reconstruction images and virtual endoscopic views using MR sialography data sets of 3D-FASE sequences are very attractive and further expansion of this field is expected.

Chapter three: conclusion and suggestions

A variety of disease patterns involve the major salivary glands with few characteristic features on imaging. high-resolution ultrasonography should be the first screening imaging tool followed by sialography, if required. CT is the mainstay of imaging in sialolithiasis while MRI is more optimal for neoplastic processes with associated invasion. CT and MRI are equally good in imaging of the cystic and inflammatory lesions especially abscesses.

The conclusion of this review of literature is to assess different type of imaging modalities for detect various disease and different type of tumors that effect parotid and submandibular salivary gland, and to focus on the important aspect of imaging the salivary gland disorders by selection of appropriate imaging method and accurate interpretation of images will help in correct diagnosis of conditions .

So, the use a combination of different type imaging such as MRI and ultrasound will result in high sensitivity, specificity, and diagnostic accuracy in characterization of tumors and conditions that effect in major and minor salivary glands.

References

-A-

-Abdel-Wahed N, Amer ME, Abo-Taleb NS. Assessment of the role of cone beam computed sialography in diagnosing salivary gland lesions. *Imaging Sci Dent.* 2013;43(1):17–23.

-Abdullah A, Rivas FF, Srinivasan A. Imaging of the salivary glands. *Semin Roentgenol.* 2013;48(1):65-74.

-Amano, O.; Mizobe, K.; Bando, Y.; Sakiyama, K. Anatomy and histology of rodent and human major salivary glands: Overview of the Japan salivary gland society-sponsored workshop. *Acta Histochem. Cytochem.* 2012, 45, 241–250. [CrossRef] [PubMed]

-B-

-Bialek EJ, Jakubowski W, Zajkowski P, Szopinski KT, Osmolski A (2006). "US of the major salivary glands: anatomy and spatial relationships, pathologic conditions, and pitfalls". *Radiographics.* 26 (3): 745–63. doi:10.1148/rg.263055024. PMID 16702452.

-Brown JE, Drage NA, Escudier MP, et al. Minimally invasive radiologically guided intervention for the treatment of salivary calculi. *Cardiovasc Intervent Radiol.* 2002;25(5):352-355.

-Browne RF, Golding SJ, Watt-Smith SR. The role of MRI in facial swelling due to presumed salivary gland disease. *Br J Radiol.* 2001;74(878):127-133.

-Burke CJ, Thomas RH, Howlett D. Imaging the major salivary glands. *Br J Oral Maxillofac Surg.* 2011;49(4):261-269.

-C-

-Chatzeli, L.; Gaete, M.; Tucker, A.S. Fgf10 and Sox9 are essential for the establishment of distal progenitor cells during mouse salivary gland development. *Development* 2017, 144, 2294–2305. [CrossRef]

-D-

- Delporte, C.; Bryla, A.; Perret, J. Aquaporins in Salivary Glands: From Basic Research to Clinical Applications. *Int. J. Mol. Sci.* 2016, 17, 166. [CrossRef]

-Dobrosielski-Vergona, K. *Biology of the Salivary Glands*; CRC Press, Taylor & Francis Group: Abingdon, UK, 1993; ISBN 978-0849388477.

-Dowd FJ. Saliva and dental caries. *Dental Clinics of North America.* 1999;43:579-597.

-Drage NA, Brown JE, Escudier MP, et al. Interventional radiology in the removal of salivary calculi. *Radiology.* 2000;214(1):139–142.

-Drage NA, Brown JE, Escudier MP, et al. Balloon dilatation of salivary duct strictures: report on 36 treated glands. *Cardiovasc Intervent Radiol.* 2002;25(5):356-359.

- Dreiseidler T, Ritter L, Rothamel D, et al. Salivary calculus diagnosis with 3-dimensional cone-beam computed tomography. *Oral Surg Oral Med Oral Pathol Oral Radiol Endod.* 2010;110(1):94–100.

-E-

- Edgar, Michael; Dawes, Colin; O'Mullane, Denis, eds. (2012). Saliva and oral health (4th ed.). Stephen Hancocks. p. 1. ISBN 978-0-9565668-3-6.
- El-Khateeb SM, Abou-Khalaf AE, Farid MM, et al. ADosimetry of 3 CBCT devices for oral and maxillofacial radiology: CB Mercuray, NewTom 3G and i-CAT. Dentomaxillofac Radiol. 2006;35(4):219-226.
- El-Rasheedy, A.El.I., Abdalla, A.M.A.R., Hassanein, S.Ah. et al. The role of ultrasound in evaluating salivary glands swellings. Egypt J Otolaryngol 37, 101 (2021). <https://doi.org/10.1186/s43163-021-00165-y>.
- Ewa J. Białek, MD, PhD, Department of Diagnostic Imaging, II Medical Division, Medical University of Warsaw, 8, 03-242 Warszawa, Poland.

-G-

- Gervais,E.M.; Sequeira, S.J.; Wang, W.; Abraham, S.; Kim, J.H.; Leonard, D.; DeSantis, K.A.; Larsen, M. Par-1b is required for morphogenesis and differentiation of myoepithelial cells during salivary gland development. Organogenesis 2016, 12, 194–216. [CrossRef]
- Groom, J.; Kalled, S.L.; Cutler, A.H.; Olson, C.; Woodcock, S.A.; Schneider, P.; Tschopp, J.; Cachero, T.G.; Batten, M.; Wheway, J.; et al. Association of BAFF/BLyS overexpression and altered B cell differentiation with Sjögren's syndrome. J. Clin. Investig. 2002, 109, 59–68. [CrossRef]
- Guntinas-Lichius, Orlando; Ihrler, Stephan; Freesmeyer, Martin; Gühne, Falk; Kluge, Regine; Bräuer, Lars; Iro, Heinrich; Paulsen, Friedrich;

Dietz, Andreas; Bechmann, Ingo (2020-11-16). "Gibt es eine neue Kopfspeicheldrüse? – Eher nicht!". *Laryngo-Rhino-Otologie* (in German). 100 (1): a–1307–3872.

-H-

- He,B.; Chadburn, A.; Jou, E.; Schattner, E.J.; Knowles, D.M.; Cerutti, A. Lymphoma B cells evade apoptosis through the TNF family members BAFF/BLyS and APRIL. *J. Immunol.* 2004, 172, 3268–3279. [CrossRef]

- Holmberg KV, Hoffman MP (2014). "Anatomy, biogenesis and regeneration of salivary glands". *Saliva: Secretion and Functions. Monographs in Oral Science. Vol. 24.* pp. 1–13. doi:10.1159/000358776. ISBN 978-3-318-02595-8. PMC 4048853. PMID 24862590.

- Hviid A, Rubin S, Mühlemann K (2008). "Mumps". *Lancet.* 371 (9616): 932–44. doi:10.1016/S0140-6736(08)60419-5. PMID 18342688. S2CID 208793825.

-I-

- Ichiro Ogura et al. *Chin J Dent Res.* Magnetic Resonance Sialography and Salivary Gland Scintigraphy of Parotid Glands in Sjögren's Syndrome,2018;21(1):63-68,https://doi.org/10.3290/j.cjdr.a39919.

-J-

- Jadu FM, Jan AM. A meta-analysis of the efficacy and safety of managing parotid and submandibular sialoliths using sialendoscopy assisted surgery. *Saudi Med J.* 2014;35(10):1188–1194.

- Jimènez-Rojo, L.; Granchi, Z.; Graf, D.; Mitsiadis, T.A. Stem Cell Fate Determination during Development and Regeneration of Ectodermal Organs. *Front. Physiol.* 2012, 3, 107. [CrossRef]

-K-

- Kondo, Y.; Nakamoto, T.; Jaramillo, Y.; Choi, S.; Catalan, M.A.; Melvin, J.E. Functional differences in the acinar cells of the murine major salivary glands. *J. Dent. Res.* 2015, 94, 715–721. [CrossRef] [PubMed]

-Korsrud, F.R.; Brandtzaeg, P. Quantitative immunohistochemistry of immunoglobulin-andJ-chain-producing cells in human parotid and submandibular salivary glands. *Immunology* 1980, 39, 129–140. [PubMed]

-M-

- MacDonald A, Burrell S. Infrequently performed studies in nuclear medicine: part 2. *J Nucl Med Technol.* 2009;37(1):1–13.

- Mandel L. Salivary gland disorders. *Med Clin North Am.* 2014;98(6):1407–1449.

- Matsuo, R. Role of saliva in the maintenance of taste sensitivity. *Crit. Rev. Oral Biol. Med.* 2000, 11, 216–229. [CrossRef] [PubMed]

-N-

- Nanci A (2018). *Ten Cate's Oral Histology: Development, Structure, and Function* (ninth ed.). ISBN 978-0-323-48524-1.

- Nahlieli O, Nazarian Y. Sialadenitis following radioiodine therapy - a new diagnostic and treatment modality. *Oral Dis.* 2006;12(5):476-479.

- Nahlieli O, Shacham R, Yoffe B, et al. Diagnosis and treatment of strictures and kinks in salivary gland ducts. *J Oral Maxillofac Surg.* 2001;59(5):484-490 [discussion 490-492].

- Ngu RK, Brown JE, Whaites EJ, et al. Salivary duct strictures: nature and incidence in benign salivary obstruction. *Dentomaxillofac Radiol.* 2007;36(2):63-67.

-O-

- Oscar Hasson. Modern sialography for screening of salivary gland obstruction, Feb 2010 Feb;68(2):276-80. doi: 10.1016/j.joms.2009.09.044.

-S-

- Senthilkumar, B.; Mahabob, M.N. Mucocele: An unusual presentation of the minor salivary gland lesion. J. Pharm. Bioallied Sci. 2012, 4 (Suppl. S2), S180–S182. [CrossRef]

- Shahidi S, Hamedani S. The feasibility of cone beam computed tomographic sialography in the diagnosis of space-occupying lesions: report of 3 cases. Oral Surg Oral Med Oral Pathol Oral Radiol. 2014;117(6):e452-e457.

- Smith, D.J.; Taubman, M.A.; King, W.F. Immunological features of minor salivary gland saliva. J. Clin. Immunol. 1987, 7, 449–455. [CrossRef] [PubMed]

-T-

- Treuting, P.M.; Dintzis, S.M.; Frevert, C.W.; Liggitt, D.; Liggitt, H.D.; Montine, K.S. Comparative Anatomy and Histology: A Mouse and Human Atlas (Expert Consult); Elsevier Inc.: UK, 2012. Available online: https://books.google.ch/books?id=Bqn23_270Q8C (accessed on 3 August 2019).

-V-

-Valstar, Matthijs H.; de Bakker, Bernadette S.; Steenbakkens, Roel J. H. M.; Vogel, Wouter V. (2020-09-22). "The tubarial salivary glands: A potential new organ at risk for radiotherapy". Radiotherapy and Oncology. 154: 292–298. doi:10.1016/j.radonc.2020.09.034. PMID 32976871.

-W-

- Wu, Katherine J. (2020-10-19). "Doctors May Have Found Secretive New Organs in the Center of Your Head". The New York Times. Retrieved 2020-10-22.

- Wilson, K.F.; Meier, J.D.; Ward, P.D. Salivary gland disorders. Am. Fam. Phys. 2014, 89, 882–888.

-Y-

- Y Morimoto et al. Oral Dis. Virtual endoscopic view of salivary gland ducts using MR sialography data from three dimension fast asymmetric spin-echo (3D-FASE) sequences: a preliminary study, 2002 Sep;8(5):268-74. <https://doi.org/10.1034/j.1601-0825.2002.01819.x>

- Yousem DM, Kraut MA, Chalian AA. Major salivary gland imaging. Radiology. 2000;216(1):19–29.